# Lattice Thermal Conductivity of Wurtzite Bulk and Zinc Blende CdSe Nanowires and Nanoplayer

Ibrahim Nazem Qader [1] & Botan Jawdat Abdullah [2] & Hawbash Hamadamin Karim [3]

[1]Department of physics, College of Science, University of Raparin, Sulaimanyah, Iraq
[2]Department of physics, College of Science, University of Salahaddin, Arbil, Iraq
[3]Department of physics, Faculty of Science and Health, University of Koya, Arbil, Iraq
Correspondence: University of Raparin, Sulaimanyah, Iraq.
E-mail: i.nazm@yahoo.com, ibrahimnazm@uor.edu.krd

Received: June 4 , 2017 Accepted: August 19, 2017 Online Published: September 1, 2017

doi: 10.23918/eajse.v3i1sip9

**Abstract: By using Morelli-Callaway model and some structure dependent parameters, theoretical calculations of LTC for wurtzite Bulk CdSe, zinc blende CdSe nanowire and nanolayer are performed. The theoretical and experimental correlation for CdSe NWs with diameter 41, 52 and 88nm and nanolayer with thickness of 4.3nm are investigated. While, the direction of growth of ZB CdSe is <110>, one equation for longitudinal and two different equation for transverse mode are used for calculating acoustic group velocity. Therefore, Morelli-Callaway model splits to three branches. There are six phonon transfer scattering rate, which are umklapp, normal, boundary impurity, dislocation, and phonon-electron scattering rate. In different temperatures, different phonon scattering process appeal. The shape of LTC as a function of temperature has a bell shape that all phonon scattering rate configured this shape. The peak of lattice thermal conductivity shift to higher temperature with decreasing the size of CdSe nanostructure. In summarize, the LTC for a particular temperature depends on the size and crystal structure. At 300K thermal conductivity of WZ bulk CdSe has less value than all ZB CdSe NWs mentioned in this work. Also quantum confinement effect cause mechanical and thermal parameters change with decreasing the size and dimension of CdSe semiconductor.**

**Keywords: Lattice Thermal Conductivity, Cdse, Phonon Scatterings, Nanowire, Nanolayer**

## 1. Introduction

The unique physical properties of cadmium selenide (CdSe) make it to become an attractive semiconductor(Grünwald, Rabani, & Dellago, 2006; Huang et al., 2007; Jia-Jin, Yan, Wen-Jun, & Qing-Quan, 2008). It provide a great bulk modulus (53.4GPa), a very low thermal conductivity (0.09 W/cm·K), wide energy gap (1.84 eV), and a high melting temperature (1623K) (Jia-Jin et al., 2008; Madelung, 2012; Omar, 2016). Three crystalline structure forms of CdSe are rocksalt (RS), wurtzite (WZ) and zincblende (ZB) structure and possibly orthorhombic or monoclinic (Jia-Jin et al., 2008; Madelung, 2012). Thermal properties are different for different structures, and different nanostructure size during quantum confinement effect (Yang et al., 2015). There are many experimental measurements of lattice thermal conductivity (LTC) for binary compound semiconductors of nanoparticles (Caylor, Coonley, Stuart, Colpitts, & Venkatasubramanian, 2005; Pernot et al., 2010), nanowires (Fon, Schwab, Worlock, & Roukes, 2002; Guthy, Nam, & Fischer,

2008; Mingo & Broido, 2004) and nanolayers (Feser, Chan, Majumdar, Segalman, & Urban, 2013; Samvedi & Tomar, 2009). In the other hand, a lot of researchers theoretically follow experimental results of LTC by applying mathematical calculation (S. Mamand, Omar, & Muhammad, 2012; S. Mamand, Omar, & Muhammed, 2012; S. M. Mamand, 2014).

In the current work lattice thermal conductivity (LTC) of bulk CdSe, single crystalline CdSe nanowires with Zinc Blende phase and nanograined film are investigated theoretically and fitted with experimental result reported by Ref. (Yang et al., 2015) and (Feser et al., 2013), respectively. Since , the growth direction is [110], then the equations are used for calculating longitudinal and transverse group velocity for bulk CdSe split Callaway model into three terms. Furthermore, the effect of dislocation, phonon-electron, boundary, phonon–phonon umklapp and normal three phonon scattering are assumed for calculation LTC for each cases that are mentioned. In addition, many size dependent parameters like mean free path, lattice constant, unit cell volume, density per atom, melting temperature, Debye temperature and acoustic group velocity are calculated. Also, there are some parameters as dislocation density, impurity, carrier concentration, surface roughness and Gruneisen parameter for each longitudinal and transverse mode that are used to fit the theoretical curve with their experimental counterparts.

## 2. Theory and Calculation

This model used by Asen-Palmer (Asen-Palmer, Bartkowski, Gmelin, & Cardona, 1997), originally formulated by Callaway J. in 1959 (Callaway, 1959). It is an important approach to study lattice thermal conductivity. The detail for LTC is given by:

$$\kappa = AT^3 \int_0^{\theta_D/T} \tau_c \, J(x) \, dx \tag{1}$$

where$A = (k_B/\hbar)^3\left(k_B/(2\pi^2 v)\right)$, $J(x) = x^4 e^x (e^x - 1)^{-2}$, $x = \hbar\omega/k_B T$, $k_B$ and $\hbar$ are the Boltzmann constant ($1.38065 \times 10^{-23}$ m$^2 \cdot$ kg $\cdot$ s$^{-2} \cdot$ K$^{-1}$) and reduced Planck constant ($1.05457 \times 10^{-23}$J $\cdot$ s), respectively, at the same time $\tau_c$ is the combined phonon relaxation time, and $v$ is acoustic group velocity, $\omega$ is the phonon angular frequency, $\theta_D$ is Debye temperature and finally $T$ is the absolute temperature, respectively.

**Table 1:** The fitting parameters of CdSe NWs used in this work for calculating LTC for each diameter.

| $r$ nm | $N_{imp}$ m$^{-3}$ | $N_D$ m$^{-2}$ | $n_e$ m$^{-3}$ | $\varepsilon$ | $L_C$ nm | $L$ μm | $\gamma_L$ | $\gamma_T$ |
|---|---|---|---|---|---|---|---|---|
| 4.3 | $4.0\times10^{26}$ | $7\times10^{16}$ | $2.5\times10^{26}$ | 0.600 | 4.3 | 4 | 0.4 | 0.3 |
| 41 | $1.0\times10^{23}$ | $10^{14}$ | $7.3\times10^{24}$ | 0.400 | 41 | 4 | 0.6 | 0.5 |
| 52 | $2.0\times10^{21}$ | $10^{14}$ | $6.8\times10^{24}$ | 0.365 | 52 | 4 | 0.68 | 0.5 |
| 88 | $2.0\times10^{21}$ | $10^{14}$ | $7.5\times10^{24}$ | 0.365 | 88 | 4 | 0.7 | 0.52 |
| Bulk | $1.0\times10^{22}$ | $10^{12}$ | $7.0\times10^{21}$ | | | | 1.3 | 0.9 |

Thermal conductivity for bulk material could be expect by using Eq. (1). Moreover, this equation can give a good theoretical calculating LTC, for of thin films (Balandin & Wang, 1998; Khitun, Balandin, & Wang, 1999) and NWs. This model has been modified by Asen-Palmer et al. (Asen-Palmer et al., 1997) Morelli et al. (D. Morelli, Heremans, & Slack, 2002) by splitting both transverse and longitudinal phonons explicitly and normal three phonon processes. Then the LTC are given by this relation (Asen-Palmer et al., 1997; D. Morelli et al., 2002):

$$\kappa = \kappa_L + 2\kappa_T \tag{2}$$

$$\kappa_L = \kappa_{L_1} + \kappa_{L_2} \tag{2a}$$

$$\kappa_T = \kappa_{T_1} + \kappa_{T_2} \tag{2b}$$

In Eq. (2a) each $\kappa_{L_1}$ and $\kappa_{L_2}$ are the standard Debye-Callaway terms which are expresed by:

$$\kappa_{L_1} = \frac{1}{3} A_L T^3 \int_0^{\theta_D^L/T} \tau_c^L(x) J(x)\, dx \tag{4}$$

$$\kappa_{L_2} = \frac{1}{3} A_L T^3 \left[\int_0^{\theta_D^L/T} \frac{\tau_c^L(x)}{\tau_N^L(x)} J(x)\, dx\right]^2 \left[\int_0^{\theta_D^L/T} \frac{\tau_c^L(x)}{\tau_N^L(x)\tau_R^L(x)} J(x)\, dx\right]^{-1} \tag{5}$$

and in similar fashion, in Eq. (2b) $\kappa_{L_1}$ and $\kappa_{L_2}$ for the transverse phonons are just like these (Omar & Taha, 2010):

$$\kappa_{T_1} = \frac{1}{3} A_T T^3 \int_0^{\theta_D^T/T} \tau_c^T(x) J(x)\, dx \tag{6}$$

$$\kappa_{T_2} = \frac{1}{3} A_T T^3 \left[\int_0^{\theta_D^T/T} \frac{\tau_c^T(x)}{\tau_N^T(x)} J(x)\, dx\right]^2 \left[\int_0^{\theta_D^T/T} \frac{\tau_c^T(x)}{\tau_N^T(x)\tau_R^T(x)} J(x)\, dx\right]^{-1} \tag{7}$$

where $T$ and $L$ in the superscripts showed the modes of each transverse and longitudinal phonons, respectively, also, $\theta_D^T$ and $\theta_D^L$ are the transverse and longitudinal Debye temperature, respectively and can be calculated by (D. Morelli et al., 2002):

$$\theta_D^{L(T)} = \left(\frac{\omega_{L(T)}\pi^2}{V}\right)^{1/3} \frac{\hbar\, v_{L(T)}}{k_B} \tag{8}$$

with $\omega_{L(T)}$is longitudinal (transverse) zone-boundary phonon frequency, also, $v_{L(T)}$is the acoustic group velocity for growth direction <110> can be calculated as (Hou, Yang, Hu, Zhang, & Yang, 2014):

$$v_L([110]) = \sqrt{\frac{1}{2}\frac{C_{11} + C_{12} + 2C_{44}}{\rho}} \tag{9a}$$

$$v_T([110]) = \sqrt{\frac{C_{44}}{\rho}} \tag{9b}$$

where $C_{11}$ , $C_{12}$ and $C_{44}$ are elastic constants, which for CdSe is given in Table (3). Furthermore, $A_L$

in Eq. (5) and $A_L$ in Eq. (7) are as follows:

$$A_L = \left(\frac{k_B}{\hbar}\right)^3 \frac{k_B}{2\pi^2 v_L} \tag{10a}$$

$$A_T = \left(\frac{k_B}{\hbar}\right)^3 \frac{k_B}{2\pi^2 v_T} \tag{10b}$$

### 2.2 Phonon-Scattering Rates

Heat transfer in semiconductor materials due to phonons effected with different scattering processes. The scattering process rate which is takes into account in the present work are: phonon–phonon (normal scattering, $\tau_N^{L(T)}$ , and anharmonic interaction or three-phonon Umklapp scattering, $\tau_U^{L(T)}$), phonon–impurity, $\tau_M^{L(T)}$, phonon–electron scattering, $\tau_{ph-e}^{L(T)}$, phonon–boundary, $\tau_B^{L(T)}$, and phonon–dislocation rate $\tau_{DC}^{L(T)}$. These scattering rate process combined as follows:

$$\left(\frac{1}{\tau_C^{L(T)}}\right) = \left(\frac{1}{\tau_N^{L(T)}}\right) + \left(\frac{1}{\tau_U^{L(T)}}\right) + \left(\frac{1}{\tau_M^{L(T)}}\right) + \left(\frac{1}{\tau_B^{L(T)}}\right) + \left(\frac{1}{\tau_{ph-e}^{L(T)}}\right) + \left(\frac{1}{\tau_{DC}^{L(T)}}\right) \tag{11}$$

The corresponding equations briefly mentioned as follows:

#### 2.2.1 Three Phonon–Phonon Umklapp and Normal Scattering Processes

Umklapp scattering (also Umklapp process or U-process), which the total of phonon wave vectors is not conserved except changes by a reciprocal lattice vector. It divided to longitudinal and transverse by (D. Morelli et al., 2002):

$$\left[\tau_U^{L(T)}\right]^{-1} = B_U^{L(T)} \left(\frac{k_B}{\hbar}\right)^2 x^2 T^3 e^{-\left(\theta_D^{L(T)}/3T\right)} \tag{12}$$

with Umklapp parameter strength for longitudinal (transverse) is given by:

$$B_U^{L(T)} = \frac{\hbar \gamma_{L(T)}^2}{M\, v_{L(T)}^2 \theta_D^{L(T)}}$$

here *M* is the average mass of an atom in the crystal, $\gamma_{L(T)}$ is Gruneisen parameter that is handled to fitting the theoretical LTC curve with corresponding experimental data.

In the other hand, normal phonon scattering has an important effect for determining the peak of the LTC (S. Mamand, Omar, & Muhammad, 2012), however it is not a resistive process (Omar & Taha, 2010). Mathematically can be expressed as:

$$\left[\tau_N^{L(T)}\right]^{-1} = B_N^{L(T)}\omega^2 T^3 \quad (13)$$

with

$$B_N^L = \frac{k_B^3 v_L^2 V}{M\hbar^3 v_L^5} \;\&\; B_N^T = \frac{k_B^4 v_T^2 V}{M\hbar^3 v_T^5}$$

where *V* is unit cell volume which is calculated for each case and listed in the Table 2.

### 2.2.2 Phonon–Impurity Scattering Rate

The atoms of a given crystal have different of mass due to present impurity or exist isotopes in its structure. The impurities specified as defects and dislocations. Also, point defects are assumed in two types, which are isotope atoms and impurity. The related relaxation rate can be expressed in term of unitless parameter, x, as shown below (S. Mamand, Omar, & Muhammad, 2012):

$$\left[\tau_M^{L(T)}\right]^{-1} = \left(I_{iso}^{L(T)} + I_{imp}^{L(T)}\right)\omega^4 \quad (14)$$

where $I_{iso}^{L(T)}$ is the phonon scattering due to different isotopes of an element or compound, and for each modes are given as:

$$I_{iso}^{L(T)} = \frac{V\,\Gamma}{4\pi\, v_{L(T)}^3}$$

likewise, $I_{imp}^{L(T)}$ is the phonon scattering distribution because of impurity, that is represented as:

$$I_{imp}^{L(T)} = \frac{3V^2\,S^2}{\pi\, v_{L(T)}^3} N_{imp}$$

here S is the scattering factor, which its value is equal to one (Klemens, 1955). In addition, $N_{imp}$ is the concentration of impurity, and can be find its value during fitting LTC curve. What is more, Γ is strength of the mass-difference scattering and for CdSe which is an alloy composed of two different elements is as follows:

$$\Gamma\,(CdSe) = 2\left[\left(\frac{M_{Cd}}{M_{Cd}+M_{Se}}\right)^2 \Gamma(Cd) + \left(\frac{M_{Se}}{M_{Cd}+M_{Se}}\right)^2 \Gamma(Se)\right] \quad (15)$$

where $M_{Cd}$ and $M_{Se}$ are the average atomic mass of *Cadmium* and *Selenide*, respectively. The coefficient of 2 in front of the square brackets is because CdSe is a binary compound (D. Morelli et al., 2002). Also, $\Gamma(Cd)$ and $\Gamma(Se)$ are the strength of the mass-difference scattering and in general form for each element can be found as:

$$\Gamma = \sum_i c_i \left(\frac{m_i - \bar{m}}{\bar{m}}\right)^2 \quad (16)$$

where $c_i$ is the percentage atomic natural abundance, $m_i$ is the atomic mass of the $i^{th}$ isotope and $\bar{m}$ is the average atomic mass is equal to $\bar{m} = \sum_i c_i m_i$. The strength for each *Cd* and *Se* isotopes is listed in Table 3.

### 2.2.3 Phonon–Boundary Scattering Rate

The phonon–boundary scattering rate for bulk is assumed self-sufficient of each frequency and temperature,

and expressed as $\left[\tau_b^{L(T)}(L)\right]^{-1} = v_{L(T)}/d$, where $d$ is the effective diameter of the specimen and is found to be 3mm due to fitting LTC at low temperature. Although, $\tau_b^{L(T)}$for nanostructures is depends on group velocity and the value of effective diameter of the sample, $L_{eff}$, however it is independent of either temperature nor frequency:

$$\left[\tau_b^{L(T)}(L)\right]^{-1} = \frac{v_{L(T)}}{L_{eff}} = v_{L(T)}\left(\frac{1}{L_c} + \frac{1}{L}\right) \tag{17}$$

**Table 2:** Calculated diameter dependence values for mean path length, Eq. (25), lattice parameter, Eq. (27), unit cell volume, Eq. (28), mass density, Eq. (29), melting temperature, Eq. (30), longitudinal and transverse Debye temperature, for nanolayer and nanowires Eq. (31) and for bulk Eq. (8). Furthermore, phonon group velocity for longitudinal and transverse, calculated for nanolayer and nanowires with Eq. (32) and for bulk is calculated by Eqs. (9a) and (9b).

| $r$ nm | $d_{mean}$ Å | α Å | V Å$^3$ | $\rho$ kg.m$^{-3}$ | $T_m$ K | $\theta_D^L$ K | $\theta_D^{T_1}$ K | $\theta_D^{T_2}$ K | $v_L$ m/s | $v_{T_1}$ m/s | $v_{T_2}$ m/s |
|---|---|---|---|---|---|---|---|---|---|---|---|
| 4.3 | 2.719 | 6.279 | 30.94 | 5164.88 | 1472.4 | 208.90 | 95.20 | 98.04 | 3715.50 | 1592.60 | 1640.5 |
| 41 | 2.649 | 6.115 | 28.58 | 5590.39 | 1593.44 | 226.11 | 112.97 | 106.10 | 3571.28 | 1530.79 | 1576.84 |
| 52 | 2.644 | 6.106 | 28.46 | 5614.60 | 1599.78 | 227.01 | 103.38 | 106.52 | 3563.57 | 1527.48 | 1573.43 |
| 88 | 2.638 | 6.093 | 28.27 | 5651.56 | 1609.36 | 228.36 | 104.00 | 107.16 | 3551.90 | 1522.48 | 1568.28 |
| Bulk | 2.630[a] | 6.074 | 28.01 | 5705.09[b] | 1623.00[a] | 230.30 | 104.89 | 108.07 | 3535.20 | 1515.32 | 1560.90 |

[a] Ref. [1010],

where L is the length of the sample. For absolute temperature smaller than Debye temperature the value of $L_{eff}$ get in order of the cross-sectional dimensions, which is known as Casimir length ($L_c$).

Furthermore, let a tiny proportion of phonons scattered because of surface of the sample, whereby, the relaxation rate of boundary scattering for longitudinal (transverse) mode is given by (Omar & Taha, 2010):

$$\left[\tau_b^{L(T)}(L,\varepsilon)\right]^{-1} = v_{L(T)}\left(\frac{1}{L_c}\frac{(1-\varepsilon)}{(1+\varepsilon)}+\frac{1}{L}\right) \tag{18}$$

Hence, $1/L_{eff}$ is specularity parameter, which is depends on the frequency of phonon and the rate of surface roughness, ε. Surface roughness has a value in the range ( 0 □□□□□□1), with maximum value (□□□1) represents phonon completely specular reflection and minimum value (□□□□0) shows the phonon is completely diffuse surface scattering.

In this work, for each CdSe NWs and nano layer the value of ε is found by fitting theoretical LTC with experimental data.

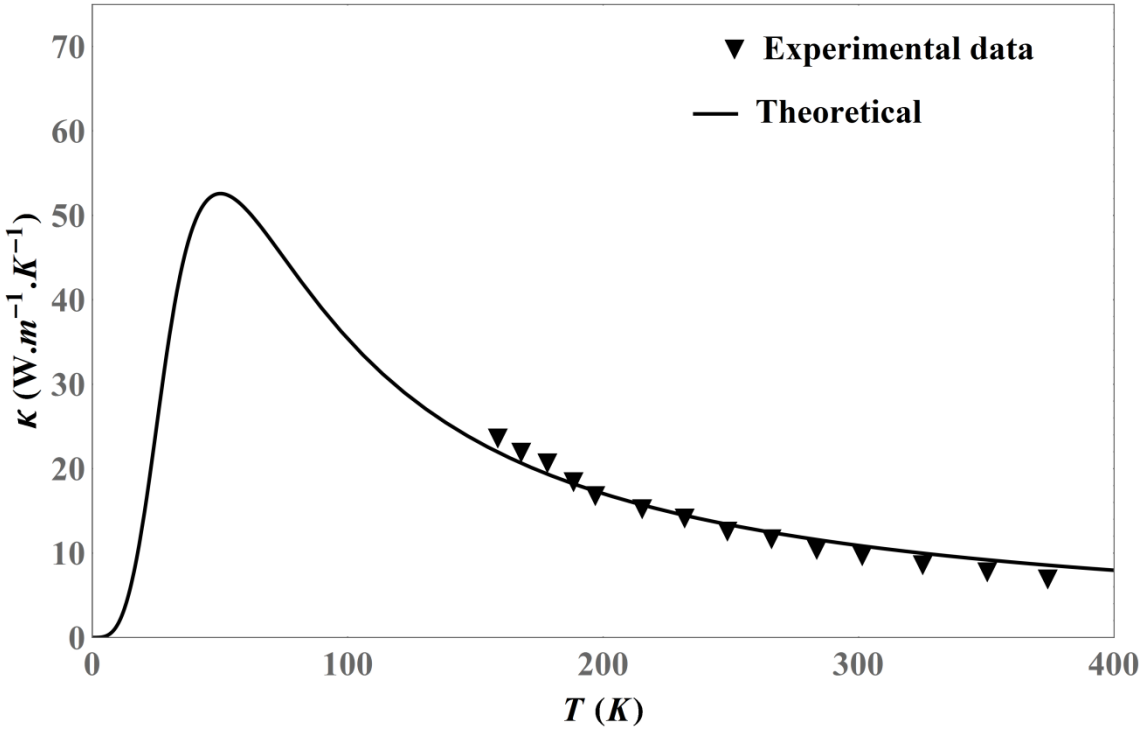


**Figure 1:** Lattice thermal conductivity of bulk CdSe as a function of temperature. The theoretical calculation (solid line) fitted experimental data (filled rectangular), Ref. (Yang et al., 2015), at high temperature and extended for low temperature.

### 2.2.4 Phonon–Dislocation Scattering Rate

The scattering of phonons due to dislocations needs to a non-linearity of phonon-dislocation interaction. Crystal including dislocation (linear defect) undergoes another phonon scattering process which is divided into short and long range scattering. The short range is similar to three-phonon Umklapp scattering, that phonons scatter on the center of the dislocation lines, moreover, the long range is scattering of phonon due to elastic strain field of dislocation lines (Jie Zou, 2010):

$$\left[\tau_{DC}^{L(T)}(x)\right]^{-1} = \eta\, N_D \frac{V_o^{4/3}}{v_{L(T)}^2}\left(\frac{k_B T}{\hbar}\right)^3 x^3 \tag{19}$$

where $\eta = 55$, that is found by integration (Klemens, 1955), is weight factor which illustrates the mutual tendency of dislocation lines and the direction of temperature gradient. Furthermore, *ND* is the density of the dislocation lines of all types. The value of dislocation density for each investigated specimens listed in Table 1.

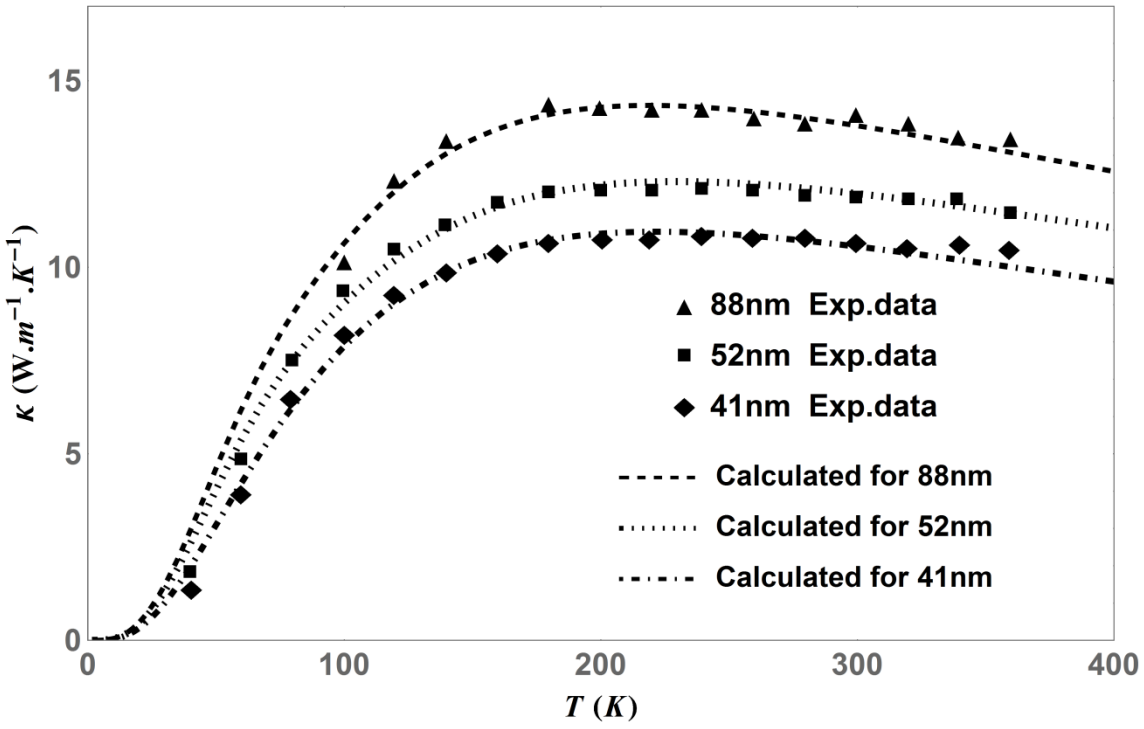


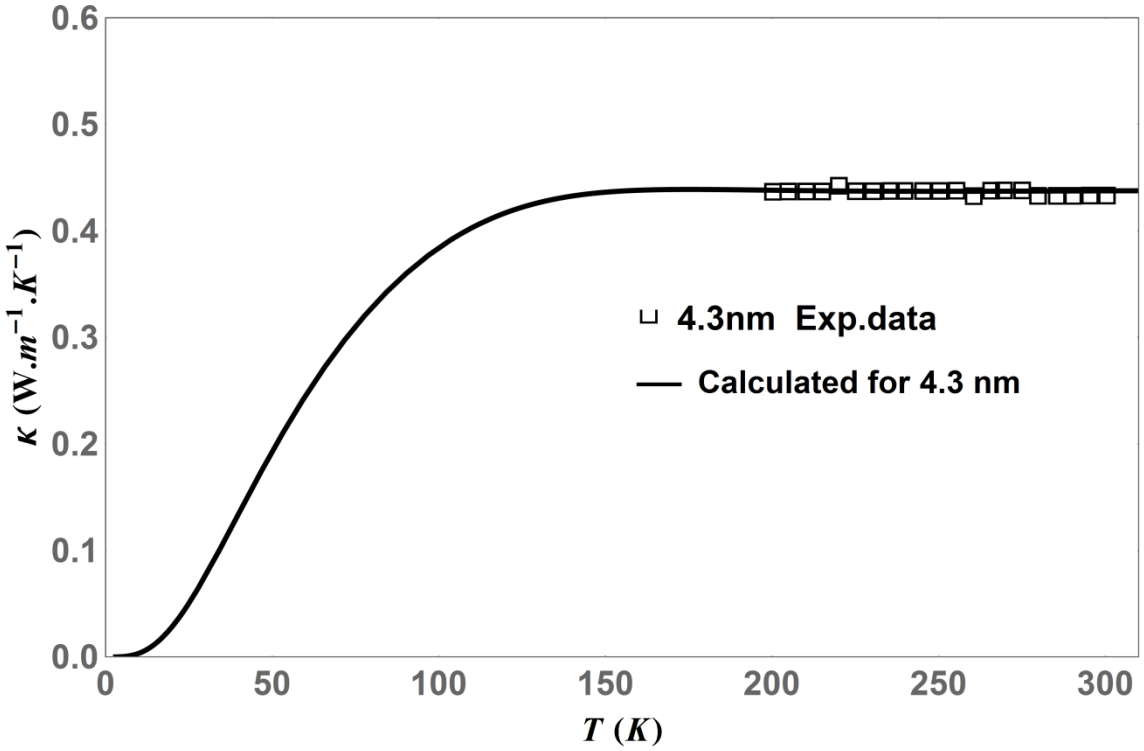

**Figure 2:** Theoretical calculation for lattice thermal conductivity of (a) zinc blonde CdSe NWs with diameters 41, 52 and 88 nm. The calculated LTC are fitted with experimental data from Ref. (Yang et al., 2015). Also, for nanolayer CdSe with thickness equal to 4.3nm is fitted (solid line) with experimental result (empty squares) reported in Ref. (Feser et al., 2013). The effect of boundary scattering is taken into account; In addition nanostructure parameters for calculating LTC assumed.

### 2.2.5 Phonon–Electron Scattering Rate

Concentration of free electron increases with increasing temperature and doped material in semiconductors. Electrons could scatter phonons, so the rate of phonon-electron scattering for each longitudinal (transverse) modes is as follows (Jie Zou & Balandin, 2001):

$$\left[\tau_{ph-e}^{L(T)}(x)\right]^{-1} = \frac{n_e E^2 x}{\rho\, v_{L(T)}^2\, \hbar} \sqrt{\frac{\pi m^* v_{L(T)}^2}{2k_B T}} \times exp\left(-\frac{m^* v_{L(T)}^2}{2k_B T}\right) \tag{20}$$

where $n_e$ is electron concentration density, $E$ is deformation potential and $\rho$ is mass density. The quantitative value for each mentioned parameters is given in Table 1-3.

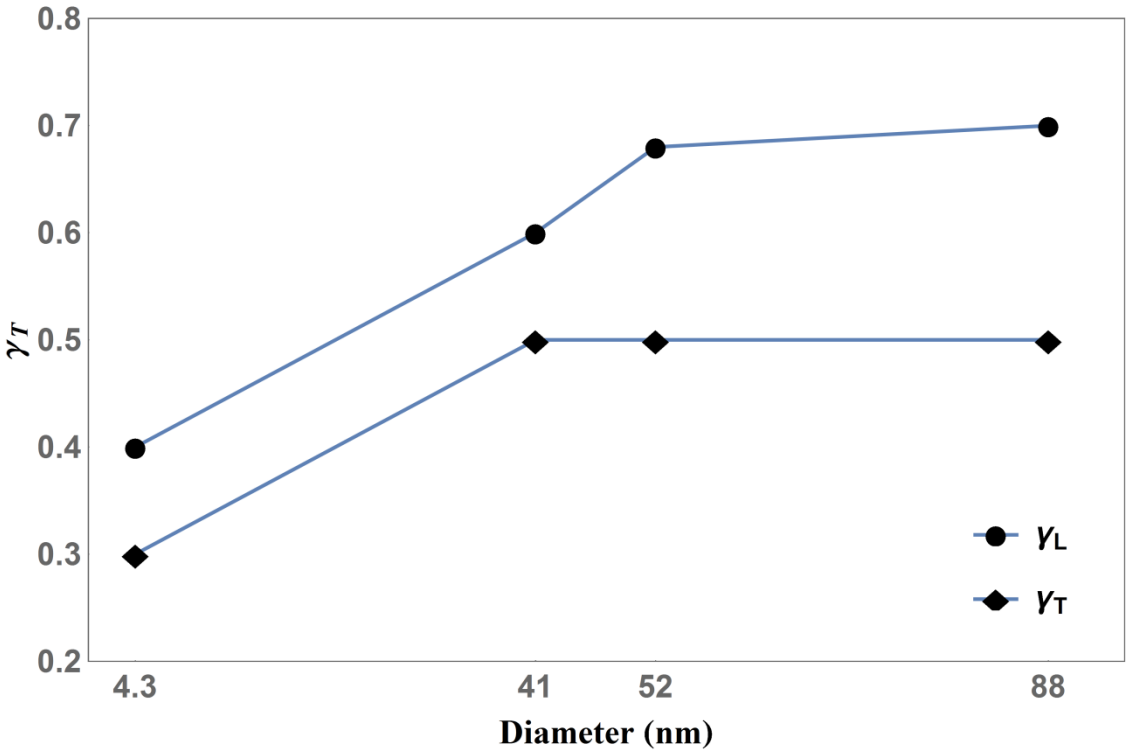


**Figure 3.** Grüneisen parameter as a function of the size which is used for fitting theoretical LTC with their corresponding experimental data of CdSe NWs and nanolayer. longitudinal and transverse Grüneisen parameter are represented as filled circle and filled square, respectively.

## 3. Lattice Thermal Conductivity of Nanostructure

To calculate LTC for nanowire (quasi -one dimension) and nanolayer (two dimension), the modification of bulk formula have to be used which include size dependent parameters. Also, the effects of acoustic phonon confinement and boundary scattering which are due to nonequilibrium phonon distribution has to be taken into account (Jie Zou & Balandin, 2001). Two factors that effect on phonon confinement are phonon dispersion and acoustic group velocity. The value of phonon group velocity decreases with decreasing size of nanostructure, that is because of quantum effect on the surface of nanostructures (Balandin & Wang, 1998; Khitun et al., 1999; Jie Zou & Balandin, 2001). Balandin and Wang (Jie Zou & Balandin, 2001) shows the role of phonon confinement on decreasing LTC of nanostructures. There is a good agreement of theoretical model for calculation of LTC, which is fitted with experimental data (S. Mamand & Omar, 2014; S. Mamand, Omar, & Muhammad, 2012; Omar & Taha, 2010) after considering the size dependent physical parameters (Omar, 2016).

In the present work each impurity density, $N_{imp}$, surface roughness, $\varepsilon$,carrier concentration, $n_e$, Gruneisen parameter, $\gamma$, lattice dislocation density, $N_D$, are found as fitting parameters, and their quantity listed in Table 1. In the other hand, mean bond length, $d_{mean}$ lattice parameter, melting temperature, $T_m$, vibrational entropy, $S_{vib}$, enthalpy of melting, $H_m$, lattice parameter, $\alpha$, unit cell volume, $V$, which are size dependent parameters, is calculated and written in Table 2.

There are two more quantities that split Callaway model into longitudinal and transverse modes, which are phonon group velocity and Debye temperature. Phonon group velocity by using mass density and elastic constants could be calculated for each modes of bulk materials (Hou et al., 2014). Similarly, Debye temperature as a function of phonon group velocity and zone-boundary phonon frequency could be calculated for longitudinal and transverse mode for bulk materials (D. Morelli et al., 2002).

### 3.1 Mean Bond Length

The value of mean bond length starts to increase when the size of crystal reduced to nano scope $d_{mean}(r)$, and this increasing get a maximum value, $d_{mean}(r_c)$, when the size of nanostructure material gets a critical size, $r_c$. The change of mean bond length for semiconductors could be calculated as follows (Omar, 2012):

$$\Delta d_{mean}(r) = \Delta d_{mean}(r_c)\left[exp\left(\frac{-2(S_m(\infty)-R)}{3R\left(\frac{r}{r_c}-1\right)}\right)\right]^{1/2} \tag{21}$$

where $R$ is ideal gas constant, and $r_c$ is depends on the dimension of nanostructure materials, $r_c = [3-D]h$, here $D$ is dimension, which for quantum dots, nanowire, nanolayer are equal to zero, one and two respectively; and h is where $h$ is the first solid surface layer height that can be calculate as:

$$h = 1.429\, d_{mean}(\infty) \tag{22}$$

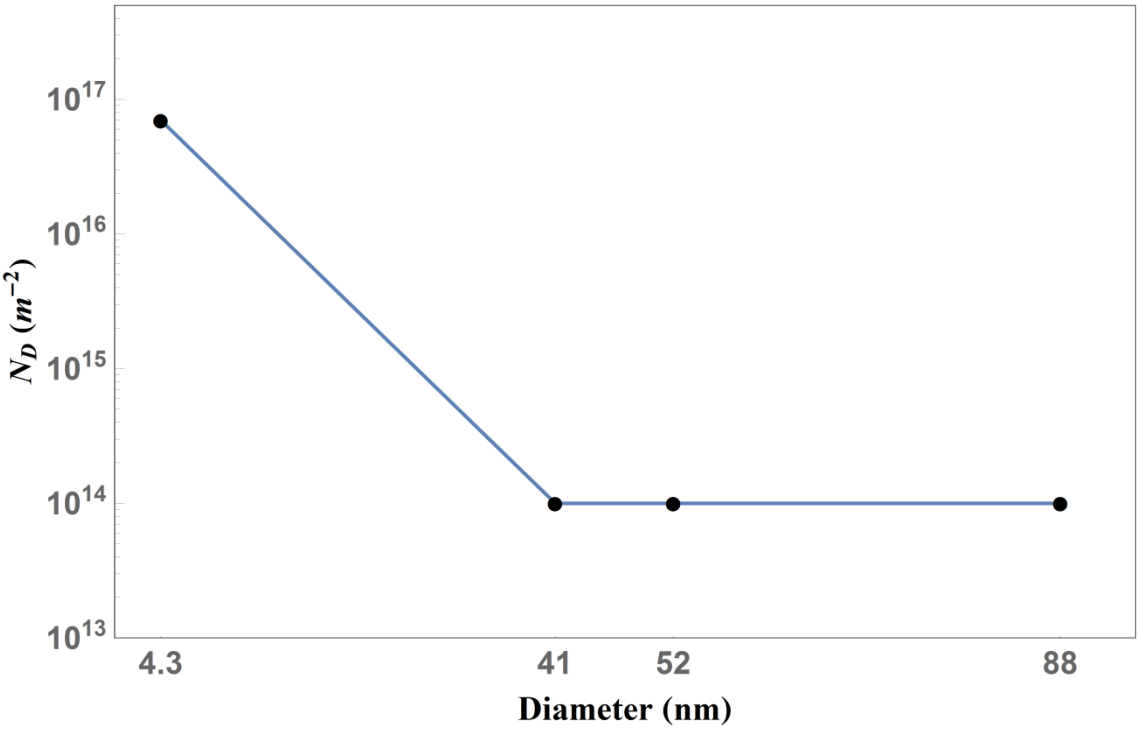


**Figure 4**: Dislocation density for CdSe nanolayer with thickness 4.3nm and NWs with diameters 41, 52 and 88nm are handled in this work to fit theoretical with experimental results.

In the Eq. (21), $S_m$is vibrational entropy for bulk and it can be find out from equation:

$$S_m(\infty) = H_m(\infty)/T_m \tag{23}$$

where $H_m(\infty)$ is the enthalpy of melting, which is function of bulk melting temperature:

$$H_m(\infty) = -10^{-5}\, T_m^2(\infty) + 0.059\, T_m(\infty) - 21.33 \tag{24}$$

Mean bond length as a function of size is as below (Omar, 2012):

$$d_{mean}(r) = h - \Delta d_{mean}(r) \tag{25}$$

Furthermore, the bulk value of $d_{mean}$ could be found as follows:

$$d_{mean}(\infty) = h - \Delta d_{mean}(r_c) \tag{26}$$

### 3.2 Lattice Constant, Unit Cell Volume and Mass Density

The physical dimensions which represent unit cell of a crystal lattice is lattice constant, whereby its quantity can be calculated as (Omar, 2007):

$$\alpha(r) = \frac{4}{\sqrt{3}} d_{mean}(r) \tag{27}$$

thus unit cell volume (Omar & Taha, 2009)

$$V(r) = \left[\frac{\alpha(r)}{2}\right]^3 \tag{28}$$

Finally, size dependence mass density of atoms is calculated from the relation:

$$\rho(r) = \frac{M}{V(r)} \tag{29}$$

### 3.3 Melting Temperature

For semiconductor material, melting temperature in as a function of size is given by (Omar, 2012):

$$\frac{T_m(r)}{T_m(\infty)} = \left(\frac{V(r)}{V(\infty)}\right)^{2/3} \exp\left[-\frac{2(S_m(\infty) - R)}{3R\left(\frac{r}{r_c} - 1\right)}\right] \tag{30}$$

Since unit cell volume for nanostructure semiconductors increases with deceasing size, then according to Eq. (30) the melting temperature decrease.

### 3.4 Debye Temperature and Lattice Group Velocity

To calculating group velocity and Debye temperature for bulk semiconductor the Eqs. (8) and (9) could be used, respectively. Thus, for nano size Debye temperature can be calculated by using Lindmann's formula (Dash, 1999; Liang & Li, 2006):

$$\left(\frac{\theta_D^n}{\theta_D^B}\right)^2 = \frac{T_m^n}{T_m^B} \tag{31}$$

In addition, the result of Debye temperature obtained from Eq. (31) could be handled to express a relationship for lattice group velocity that is extracted from Post (Post, 1953) assumption of isotropic system is as following

$$\frac{v^n}{v^B} = \frac{\theta_D^n}{\theta_D^B} \tag{32}$$

Basic parameters for CdSe are listed in Table 3. Also, the outcomes of calculation of for each CdSe NWs and nanolayer with diameter 41nm, 52nm, 88nm 4.3nm listed in Table 2.

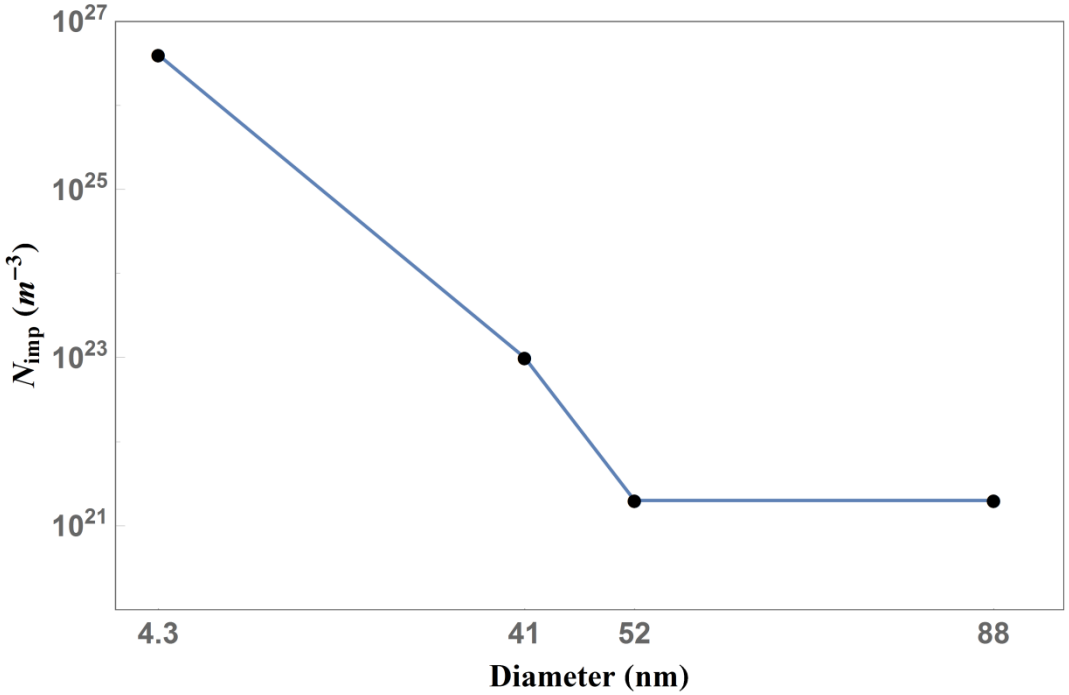


**Figure 5**: Impurity densities for thickness and diameter of 4.3, 41, 52 and 88nm are found for each CdSe nanolayer and NWs, respectively. The quantitative value increases with decreasing nanostructure size.

**Table 3:** Material parameters of CdSe

| | | | |
|---|---|---|---|
| Ideal gas constant | $R$ | $8.314(J.K^{(-1)}.mol^{(-1)})$ | Ref. (Omar, 2016) |
| First surface layer height | $h$ | 0.375827 (nm) | From Eq. (20) |
| Enthalpy of fusion | $H_m$ | 48.1 ($J.mol^{-1}$) | From Eq. (22) |
| Bulk overall melting entropy | $S_m(\infty)$ | $29.63\times10^{-4}$($J.K^{-1}.mol^{-1}$) | From Eq. (21) |
| Average atomic mass | A | 95.68 amu | Ref. (D. T. Morelli & Slack, 2006) |
| Mass per atom | $M$ | $1.6\times10^{-25}$ (kg) | Ref. (D. T. Morelli & Slack, 2006) |
| Strength of the mass-difference scattering | $\Gamma$ | $3.45\times10^{-4}$ | |
| Cd isotopes | | 1.25% $^{106}$Cd<br>0.89% $^{108}$Cd<br>12.5% $^{110}$Cd<br>12.8% $^{111}$Cd<br>24.1% $^{112}$Cd<br>12.2% $^{113}$Cd<br>28.7% $^{114}$Cd<br>7.49% $^{116}$Cd | Ref. (Wombacher, Rehkämper, Mezger, & Münker, 2003) |

| | | | |
|---|---|---|---|
| Se isotopes | | 0.89% $^{74}Se$<br>9.36% $^{76}Se$<br>7.63% $^{77}Se$<br>23.78% $^{78}Se$<br>49.61% $^{80}Se$<br>8.73% $^{82}Se$ | Ref. (Rouxel, Ludden, Carignan, Marin, & Fouquet, 2002) |
| *Elastic constants* | $C_{11}$<br>$C_{12}$<br>$C_{44}$ | 70.5 GPa<br>44.3 GPa<br>13.9 GPa | Ref. (Hou et al., 2014) |
| zone-boundary phonon frequency | $\omega_L$<br>$\omega_T$ | $211\ cm^{-1}$<br>$169\ cm^{-1}$ | Ref. (Adachi, 2004) |
| Weight factor | $\eta$ | 0.55 | Ref. (J Zou, Kotchetkov, Balandin, Florescu, & Pollak, 2002) |
| Deformation potential | $E_n$ | 4.25 (eV) | Ref. (Madelung, 2004) |
| Effective mass | $m^*$ | 0.112 $m_e$ | Ref. (Madelung, 2004) |

## 4. Analysis of Results

### 4.1 LTC in Bulk CdSe

Morelli-Callaway model (D. Morelli et al., 2002), which is a modification of last version of Callaway model (Callaway, 1959), is applied to calculate LTC as a function of temperature for bulk CdSe. The correlated of theoretical and experimental data is depicted in Fig. (1). The curve include high, intermediate and low temperature regions. The theoretical calculation has a good agreement with experimental data in high temperature region.

To fit the LTC some adjustable parameters, that are written in Table. 1, are used. In addition, by using elastic constants and given equations in Ref. (Hou et al., 2014; D. Morelli et al., 2002), longitudinal and transverse Debye temperature and acoustic group velocity for bulk CdSe are calculated and with the other parameters are listed in Table (2). To complete calculation of LTC some specific material parameters are given in Table (3).

### 4.2 LTC of CdSe NWs and Nanolayer

The correlated of theoretical and experimental of LTC for CdSe NWs with diameter 41,52 and 88nm and nanolayer with thickness 4.3nm are depicted in figure (2a) and (2b), respectively. At low temperature ($T < 50K$), all LTC related to $T^3$. The maximum values of LTC and their corresponding temperature depend on the diameter of NWs and thickness of nanolayer.

Since, the quantitative value for each impurity, dislocation density, carrier concentration, surface roughness, Casimir length and Gruneisen parameters were not measured for CdSe, then they

assumed as adjustable parameters and have found by fitting curves of LTC with their related experimental results and given in Table (1).

By using Eqs. (1) to (20), LTC were calculated and Eqs. (21) to (32), which are size dependent parameters, has been used for NWs and nanolayer CdSe. The value for mean path length, lattice constant, unit cell volume, mass density, melting temperature, longitudinal and transverse of Debye temperature and group velocity, are listed in Table (2).

The shape of LTC is due to relaxation rates. At low temperature boundary and phonon–electron scattering rate, at moderate temperature impurity and dislocation relaxation rates, and at high temperature umklapp scattering have significant effect on LTC. For nanolayer, LTC from 150K to 300K is very flat, because scattering rate is constant and has a slight frequency dependence, like boundary scattering.

At room temperature LTC of bulk CdSe, that has wurtzite (WZ) crystal, has lower value than zinc blende CdSe with all diameter mentioned in this work for nanowires. However, the LTC of NWs of WZ CdSe with lateral dimensions of (342nm × 172nm) and (330nm × 174nm) at 300K are even lower than ZB CdSe with diameter 41nm (Yang et al., 2015). The reduced LTC in WZ CdSe is due to the number of basis in crystal lattice, which are higher than ZB phase structure. Furthermore, WZ has higher anharmonicity compared to the ZB phase.

Fitting parameters have been used in the current work as a function of size are shown in Fig. (3) to (7) for Grüneisen parameter, dislocation density, impurity density, carrier concentration and surface roughness, respectively. Grüneisen parameter decrease with decreasing the nanostructures size in fig. (3) for each longitudinal and transverse modes. While, in the other parameters have significant increasing with decreasing nanoscale size.

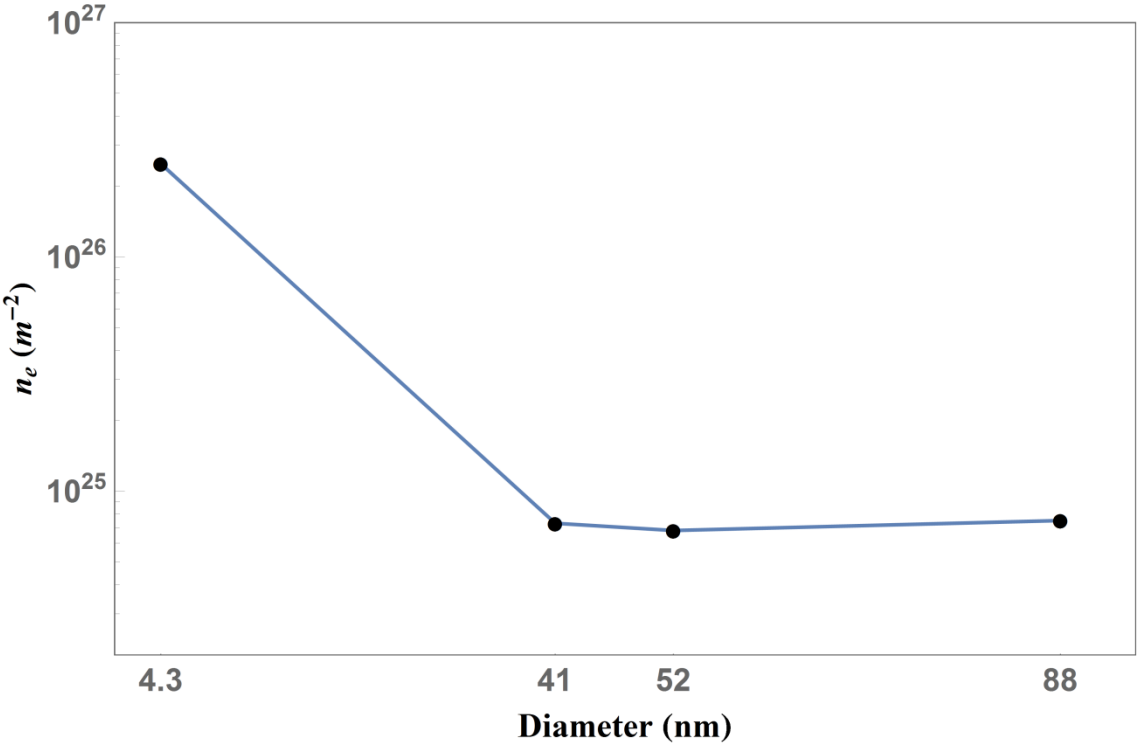

**Figure 6:** carrier concentration as a function of thickness of nanolayer and diameter of CdSe NWs, which are used for fitting calculated LTC in the current work for each 4.3, 41, 52 and 88nm.

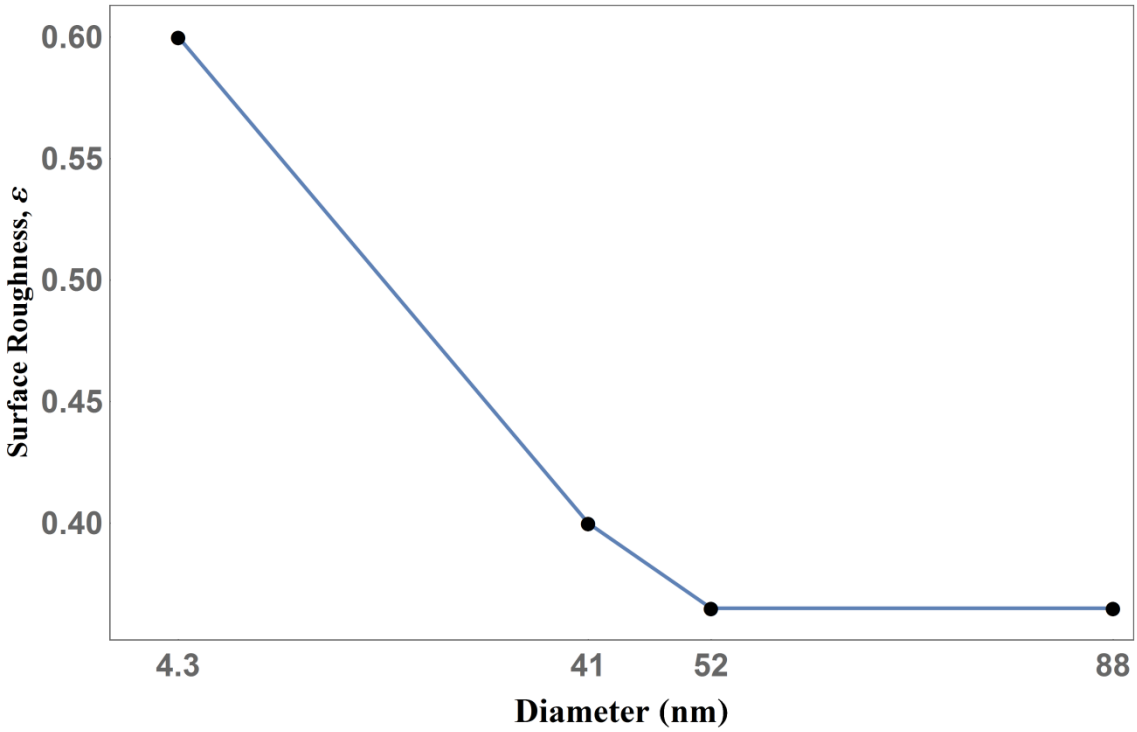


**Figure 7:** Surface roughness for CdSe NWs with diameter 41, 52, 88nm and CdSe nanolayer with 4.3nm thick are used as fitting parameters in this work.

## 5. Conclusions

Theoretical calculations of LTC for Bulk CdSe are performed by using Morelli-Callaway model. Since the direction of growth of ZB CdSe is <110>, the equations used for calculating acoustic group velocity splits to one equation for longitudinal and two different equation for transverse mode. Thus, to calculate LTC for ZB CdSe the Morelli-Callaway model splits to three branches.

There are six phonon scattering process that are influence the heat transfer in CdSe and their effects are temperature range dependence. All effects mentioned shape LTC curve, where LTC has a dramatically increasing in low temperature region and gets a maximum value then make an exponential decrease in high temperature region.

The same calculation are executed for CdSe NWs with diameter 41, 52 and 88nm and nanolayer with thickness of 4.3nm. There are some parameters that are calculated by using size dependent equations. Parameters like mean free path, lattice parameter, unit cell volume and acoustic group velocity their quantitative values rise with decreasing size of CdSe; However, melting temperature and Debye temperature decrease with reduce the size of CdSe nanowire and nanolayer. In addition, the value of dislocation density, impurity, carrier concentration, and surface roughness found by using fitting the

curves and their values increase with decreasing nanostructures size. Likewise, Grüneisen parameter for each longitudinal and transverse modes used as adjustable parameter and their values step down with decreasing the size of CdSe NWs and nanolayer.

In general, LTC for a given temperature depends on the size and crystal structure of CdSe nanostructure. At room temperature thermal conductivity of WZ bulk CdSe has lower value than all ZB CdSe NWs mentioned in the current work.

**References**

Adachi, S. (2004). *Handbook on physical properties of semiconductors* (Vol. 2): Springer Science & Business Media.

Asen-Palmer, M., Bartkowski, K., Gmelin, E., & Cardona, M. (1997). AP Zhernov, AV Inyushkin, A. Taldenkov, and VI Ozhogin, KM Itoh and EE Haller. *Phys. Rev. B, 56*, 9431-9447.

Balandin, A., & Wang, K. L. (1998). Significant decrease of the lattice thermal conductivity due to phonon confinement in a free-standing semiconductor quantum well. *Physical Review B, 58*(3), 1544.

Callaway, J. (1959). Model for lattice thermal conductivity at low temperatures. *Physical Review, 113*(4), 1046.

Caylor, J., Coonley, K., Stuart, J., Colpitts, T., & Venkatasubramanian, R. (2005). Enhanced thermoelectric performance in PbTe-based superlattice structures from reduction of lattice thermal conductivity. *Applied physics letters, 87*(2), 023105.

Dash, J. (1999). History of the search for continuous melting. *Reviews of Modern Physics, 71*(5), 1737.

Feser, J. P., Chan, E. M., Majumdar, A., Segalman, R. A., & Urban, J. J. (2013). Ultralow thermal conductivity in polycrystalline CdSe thin films with controlled grain size. *Nano letters, 13*(5), 2122-2127.

Fon, W., Schwab, K., Worlock, J., & Roukes, M. (2002). Phonon scattering mechanisms in suspended nanostructures from 4 to 40 K. *Physical Review B, 66*(4), 045302.

Grünwald, M., Rabani, E., & Dellago, C. (2006). Mechanisms of the wurtzite to rocksalt transformation in CdSe nanocrystals. *Physical review letters, 96*(25), 255701.

Guthy, C., Nam, C.-Y., & Fischer, J. E. (2008). Unusually low thermal conductivity of gallium nitride nanowires. *Journal of Applied Physics, 103*(6), 064319.

Hou, H., Yang, J., Hu, F., Zhang, S., & Yang, S. (2014). Structural, elastic and thermodynamic properties of rock-salt structure CdSe at high temperature and high pressure,". *Chalcogenide letters, 11*(3), 121-128.

Huang, S.-P., Cheng, W.-D., Wu, D.-S., Hu, J.-M., Shen, J., Xie, Z., . . . Gong, Y.-J. (2007). Density functional theoretical determinations of electronic and optical properties of nanowires and bulks for CdS and CdSe. *Applied physics letters, 90*(3), 031904.

Jia-Jin, T., Yan, C., Wen-Jun, Z., & Qing-Quan, G. (2008). Elastic and thermodynamic properties of CdSe from first-principles calculations. *Communications in Theoretical Physics, 50*(1), 220.

Khitun, A., Balandin, A., & Wang, K. (1999). Modification of the lattice thermal conductivity in silicon quantum wires due to spatial confinement of acoustic phonons. *Superlattices and microstructures, 26*(3), 181-193.

Klemens, P. (1955). The scattering of low-frequency lattice waves by static imperfections. *Proceedings of the Physical Society. Section A, 68*(12), 1113.

Liang, L., & Li, B. (2006). Size-dependent thermal conductivity of nanoscale semiconducting systems. *Physical Review B, 73*(15), 153303.

Madelung, O. (2004). II-VI compounds *Semiconductors: Data Handbook* (pp. 173-244): Springer.

Madelung, O. (2012). *Semiconductors: data handbook*: Springer Science & Business Media.

Mamand, S., & Omar, M. (2014). *Effect of Parameters on Lattice Thermal Conductivity in*

*Germanium Nanowires.* Paper presented at the Advanced Materials Research.
Mamand, S., Omar, M., & Muhammad, A. (2012). Nanoscale size dependence parameters on lattice thermal conductivity of Wurtzite GaN nanowires. *Materials Research Bulletin, 47*(5), 1264-1272.
Mamand, S., Omar, M., & Muhammed, A. (2012). Calculation of lattice thermal conductivity of suspended GaAs nanobeams: Effect of size dependent parameters. *Adv Mat Lett, 3*(6), 449-458.
Mamand, S. M. (2014). Phonon scatterings in the lattice thermal conductivity of alloy nanowires: Theoretical study. *American Journal of Nanoscience and Nanotechnology, 2*(2), 21-27.
Mingo, N., & Broido, D. (2004). Lattice thermal conductivity crossovers in semiconductor nanowires. *Physical review letters, 93*(24), 246106.
Morelli, D., Heremans, J., & Slack, G. (2002). Estimation of the isotope effect on the lattice thermal conductivity of group IV and group III-V semiconductors. *Physical Review B, 66*(19), 195304.
Morelli, D. T., & Slack, G. A. (2006). High lattice thermal conductivity solids *High thermal conductivity materials* (pp. 37-68): Springer.
Omar, M. (2007). Lattice thermal expansion for normal tetrahedral compound semiconductors. *Materials Research Bulletin, 42*(2), 319-326.
Omar, M. (2012). Models for mean bonding length, melting point and lattice thermal expansion of nanoparticle materials. *Materials Research Bulletin, 47*(11), 3518-3522.
Omar, M. (2016). Structural and Thermal Properties of Elementary and Binary Tetrahedral Semiconductor Nanoparticles. *International Journal of Thermophysics, 37*(1), 1-11.
Omar, M., & Taha, H. (2009). Lattice dislocation in Si nanowires. *Physica B: Condensed Matter, 404*(23), 5203-5206.
Omar, M., & Taha, H. (2010). Effects of nanoscale size dependent parameters on lattice thermal conductivity in Si nanowire. *Sadhana, 35*(2), 177-193.
Pernot, G., Stoffel, M., Savic, I., Pezzoli, F., Chen, P., Savelli, G., . . . Mönch, I. (2010). Precise control of thermal conductivity at the nanoscale through individual phonon-scattering barriers. *Nature materials, 9*(6), 491-495.
Post, E. (1953). On The Characteristic Temperatures of Single Crystals and the Dispersion of the " Debye Heat Waves". *Canadian Journal of Physics, 31*(1), 112-119.
Rouxel, O., Ludden, J., Carignan, J., Marin, L., & Fouquet, Y. (2002). Natural variations of Se isotopic composition determined by hydride generation multiple collector inductively coupled plasma mass spectrometry. *Geochimica et Cosmochimica Acta, 66*(18), 3191-3199.
Samvedi, V., & Tomar, V. (2009). The role of interface thermal boundary resistance in the overall thermal conductivity of Si–Ge multilayered structures. *Nanotechnology, 20*(36), 365701.
Wombacher, F., Rehkämper, M., Mezger, K., & Münker, C. (2003). Stable isotope compositions of cadmium in geological materials and meteorites determined by multiple-collector ICPMS. *Geochimica et Cosmochimica Acta, 67*(23), 4639-4654.
Yang, J., Tang, H., Zhao, Y., Zhang, Y., Li, J., Ni, Z., . . . Xu, D. (2015). Thermal conductivity of zinc blende and wurtzite CdSe nanostructures. *Nanoscale, 7*(38), 16071-16078.
Zou, J. (2010). Lattice thermal conductivity of freestanding gallium nitride nanowires. *Journal of Applied Physics, 108*(3), 034324.
Zou, J., & Balandin, A. (2001). Phonon heat conduction in a semiconductor nanowire. *Journal of Applied Physics, 89*(5), 2932-2938.
Zou, J., Kotchetkov, D., Balandin, A., Florescu, D., & Pollak, F. H. (2002). Thermal conductivity of GaN films: Effects of impurities and dislocations. *Journal of Applied Physics, 92*(5), 2534-2539.